Report

Current Biology

Viruses Inhibit CO_2 Fixation in the Most Abundant Phototrophs on Earth

Highlights

- Viruses of abundant marine cyanobacteria shut down CO_2 fixation during infection
- The strength of the shutdown is dependent on the viral gene content
- Viruses encoding genes that actively shut down CO_2 fixation are less productive

Authors

Richard J. Puxty, Andrew D. Millard, David J. Evans, David J. Scanlan

Correspondence

d.j.scanlan@warwick.ac.uk

In Brief

Puxty et al. show that marine cyanobacterial viruses modify host photosynthesis to maximize energy production but inhibit CO_2 fixation. These phototrophs are responsible for ~10% of global CO_2 fixation, and up to 60% of cells are infected at any time. Therefore, this phenomenon has implications for the assessment of primary production of the biosphere.

Puxty et al., 2016, Current Biology *26*, 1–5
June 20, 2016
http://dx.doi.org/10.1016/j.cub.2016.04.036

CellPress

Please cite this article in press as: Puxty et al., Viruses Inhibit CO_2 Fixation in the Most Abundant Phototrophs on Earth, Current Biology (2016), http://dx.doi.org/10.1016/j.cub.2016.04.036

Current Biology
Report

Viruses Inhibit CO_2 Fixation in the Most Abundant Phototrophs on Earth

Richard J. Puxty,[1,2] Andrew D. Millard,[3,5] David J. Evans,[4] and David J. Scanlan[1,5,*]
[1]School of Life Sciences, University of Warwick, West Midlands CV4 7AL, UK
[2]Department of Ecology and Evolutionary Biology, University of California, Irvine, Irvine, CA 92697, USA
[3]Warwick Medical School, University of Warwick, West Midlands CV4 7AL, UK
[4]Biomedical Sciences Research Complex, North Haugh, University of St Andrews, Fife KY16 9ST, UK
[5]Co-senior author
*Correspondence: d.j.scanlan@warwick.ac.uk
http://dx.doi.org/10.1016/j.cub.2016.04.036

SUMMARY

Marine picocyanobacteria of the genera *Prochlorococcus* and *Synechococcus* are the most numerous photosynthetic organisms on our planet [1, 2]. With a global population size of 3.6×10^{27} [3], they are responsible for approximately 10% of global primary production [3, 4]. Viruses that infect *Prochlorococcus* and *Synechococcus* (cyanophages) can be readily isolated from ocean waters [5–7] and frequently outnumber their cyanobacterial hosts [8]. Ultimately, cyanophage-induced lysis of infected cells results in the release of fixed carbon into the dissolved organic matter pool [9]. What is less well known is the functioning of photosynthesis during the relatively long latent periods of many cyanophages [10, 11]. Remarkably, the genomes of many cyanophage isolates contain genes involved in photosynthetic electron transport (PET) [12–18] as well as central carbon metabolism [14, 15, 19, 20], suggesting that cyanophages may play an active role in photosynthesis. However, cyanophage-encoded gene products are hypothesized to maintain or even supplement PET for energy generation while sacrificing wasteful CO_2 fixation during infection [17, 18, 20]. Yet this paradigm has not been rigorously tested. Here, we measured the ability of viral-infected *Synechococcus* cells to fix CO_2 as well as maintain PET. We compared two cyanophage isolates that share different complements of PET and central carbon metabolism genes. We demonstrate cyanophage-dependent inhibition of CO_2 fixation early in the infection cycle. In contrast, PET is maintained throughout infection. Our data suggest a generalized strategy among marine cyanophages to redirect photosynthesis to support phage development, which has important implications for estimates of global primary production.

RESULTS AND DISCUSSION

First, we assessed CO_2 uptake at a fixed irradiance. At 30 μmol photons m^{-2} s^{-1}, uninfected *Synechococcus* sp. WH7803 fixed CO_2 linearly throughout the experimental period (Figure 1A). Infection with cyanophage S-PM2d resulted in cessation of CO_2 fixation ~4 hr after infection (Figure 1A) (approximately 1/3 of the latent period; Figure 3A) [10]. Similarly, infection with cyanophage S-RSM4 results in cessation of CO_2 fixation, but much earlier during infection (~2 hr; Figure 1A). This is despite a longer latent period in this cyanophage (~15 hr; Figure 3A). While there is a clear difference in CO_2 fixation capacity between infected and uninfected cells and between infections with different phages, this may be imparted by modifications to the photosynthetic electron transport (PET) machinery by the infecting phage that cause a shift in the light response curve of photosynthesis. Therefore, we assessed CO_2 uptake over a light gradient in a "photosynthetron" [21] (Figure 1B). These data show that under all light irradiances there is a reduced CO_2 fixation rate in cells infected with either S-PM2d or S-RSM4 compared with uninfected cells. Interestingly, we did observe a slight broadening of the irradiance at which the maximal rate of photosynthesis (P_{max}) occurs in cells infected with S-PM2d, which may indicate modification of the photosynthetic apparatus by phage gene products.

To detect any changes in the light-dependent reactions of photosynthesis, we assessed the quantum yield of PSII photochemistry (F_v/F_m) between uninfected cells or cells infected with either cyanophage. Over a time series, this measurement determines the rate of re-oxidation of the primary acceptor of PSII by downstream photochemical processes. In contrast to CO_2 fixation, we could not detect any significant changes in F_v/F_m between uninfected *Synechococcus* and *Synechococcus* infected with either cyanophage (Figure 2). This indicates that PET was stable during the infection period and presumably supplies energy in the form of ATP and reducing power to phage morphogenesis [20].

We hypothesized that the more pronounced cessation of CO_2 fixation in S-RSM4 compared with S-PM2d would manifest as an increase in phage productivity. Therefore, we conducted comparative one-step growth experiments between these cyanophages (Figure 3). We demonstrate that, in fact, S-PM2d has both a shorter latent period than S-RSM4 (12 hr versus 14 hr, respectively; Figure 3A) and a larger burst size (2.15-fold, range = 1.52–3.90). These differences are reflected in comparative rates of plaque growth (Figures 3A and 3B), with S-PM2d producing 3.21-fold larger plaques over a 10-day period (one-way ANOVA, $F_{1,88} = 513.17$, $p < 0.001$).

Previous studies, prior to the genomic era and uninformed about virus-encoded photosynthesis gene products, have produced

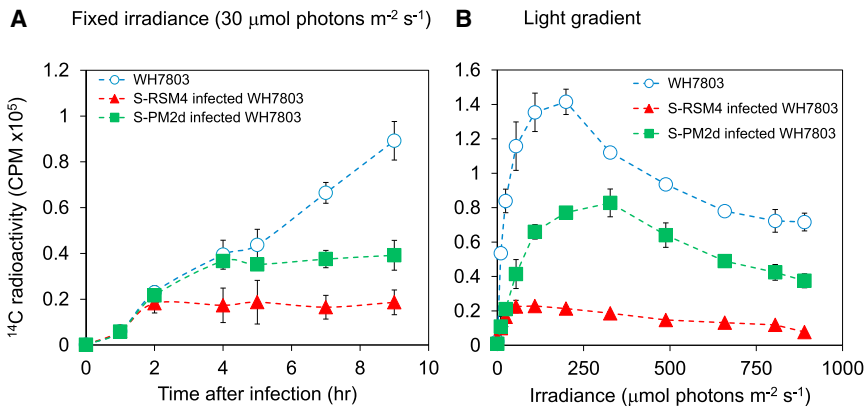

Figure 1. Effect of Viral Infection on $NaH^{14}CO_3$ Uptake by *Synechococcus* sp. WH7803

(A) $NaH^{14}CO_3$ uptake over time at a fixed irradiance (30 μmol photons m^{-2} s^{-1}).

(B) $NaH^{14}CO_3$ uptake over a light gradient for the first 5 hr post infection. Error bars signify the SD of three biological replicates.

contradictory data on CO_2 fixation by cyanophage-infected freshwater cyanobacteria [22–24]. Therefore, in light of this realization, we revisited some of these experiments in a cyanobacterium of global importance. Our data clearly demonstrate, for the first time, a viral-induced inhibition of CO_2 fixation during infection of marine *Synechococcus*. This strongly implies that the cell contains ample carbon resources, but that the ATP and reducing power generated by PET are needed for virus morphogenesis, an interpretation reinforced by inhibitor studies of photosystem II functioning [25]. We suggest that the cessation of CO_2 fixation early in the infection period by S-RSM4 compared with S-PM2d is the result of the maintenance of central carbon metabolism genes in S-RSM4 (Table 1). S-RSM4 contains orthologs of the genes *talC* (host *talB*), *cp12*, *zwf*, and *gnd* [19]. CP12 is an inhibitor of the Calvin cycle enzymes phosphoribulokinase (*prkB*, consuming 1 ATP) and GADPH (*gap2*, consuming 1 NADPH) [28]. CP12 has been shown to inhibit CO_2 fixation and regulates the photosynthetic response to the transition to the daily dark period experienced by picocyanobacteria [28–30]. Meanwhile, the transaldolase *talC* is shared by both the Calvin cycle and the pentose phosphate pathway (PPP) but is the only enzyme that operates in the direction of the PPP and against the direction of the Calvin cycle [31]. *zwf* and *gnd* are components of the PPP, whereby the activities of both generate NADPH [20]. The combined activities of these gene products have been suggested to bolster the PPP during infection for phage dNTP synthesis [20]. This hypothesis is reinforced by evidence that these genes are expressed during infection [20], that phage gene products are functional in vitro [20], and that cyanophage infection augments the dynamics of NADPH and its derivatives [20]. Our data support this hypothesis given that a cyanophage encoding C metabolism genes seems to inhibit CO_2 fixation more rapidly than a cyanophage lacking them. We hypothesize that evolution has selected for the maintenance of genes that inhibit CO_2 fixation in cyanophages, and thus the decreased productivity of S-RSM4 compared with S-PM2d was unexpected. However, our data are limited to laboratory conditions and therefore exclude environmental factors likely experienced by cyanophages in nature, e.g., a diel light regime and/or nutrient limitation. Certainly, comparative metagenomics has revealed differing representation of *zwf*, *gnd*, and *cp12* sequences in Mediterranean, Pacific, and Atlantic water column samples [32]. Hence, further work is required to dissect the role of specific environmental parameters in the productivity and CO_2 fixation capacities of cells infected with different cyanophage strains.

Another explanation for the observed decrease in CO_2 fixation by infected cells is an increase in carbon-loss processes, e.g., enhanced respiration or dissolved organic carbon production. In light of the evidence surrounding the cessation of host metabolism in other phage-host systems [33], the maintenance of genes encoding PET components in cyanophages, and the observed changes in CO_2 fixation between the two phages studied here, we favor our first hypothesis. However, although we cannot exclude such carbon-loss processes, we still note that regardless of the mechanism, phage-infected cells fix less net CO_2.

Assuming *Prochlorococcus* and *Synechococcus* contribute approximately 10% of global net primary production [3, 4], a mean global day length of 12 hr, cyanophage latent periods between 6 and 15 hr [10, 11] (Figure 3), cessation of CO_2 fixation between 20% and 50% (of the latent period), and between 1% and 60% of cells being infected per day [34–36], we estimate between 0.02 and 5.39 Pg C per year is lost to viral-induced inhibition of CO_2 fixation. The upper figure of this range represents approximately 2.8-fold greater productivity than the sum of all coral reefs, salt marshes, estuaries, and marine macrophytes on Earth [37]. Moreover, with climate change predicted to expand both the oceanic gyre regimes [38, 39] and the abundance of picocyanobacteria [3], the impact of cyanophages on global CO_2 fixation is expected to increase. To better quantify this impact, it is essential to develop improved measurements of infection rates in wild populations of prokaryotic picophytoplankton as well as the effects of biotic factors on the infection process.

Our data also have important implications for the measurement of CO_2 fixation in marine ecosystems. Methods to track changes in the estimation of net primary production and, in particular, group-specific gross CO_2 fixation rates are often laborious, expensive, and allow for poor resolution [40]. Recent attention has focused on developing proxies for CO_2 fixation rates derived from in situ fluorescence-based measurements of photochemistry [41]. Although these methods provide greater spatial and temporal resolution, they rely on strict coupling of the light reactions of photosynthesis to CO_2 fixation. We show here that the latter assumption is incorrect. Instead, cyanophage development acts as a sink of PSII-derived electrons, diverting them away from the Calvin cycle and thus effectively decoupling the light and dark reactions of photosynthesis. This is likely particularly important for ocean gyre regimes, where *Prochlorococcus* is the dominant component of the photosynthetic community [2, 3]. Indeed, fluorescence-based estimates of primary

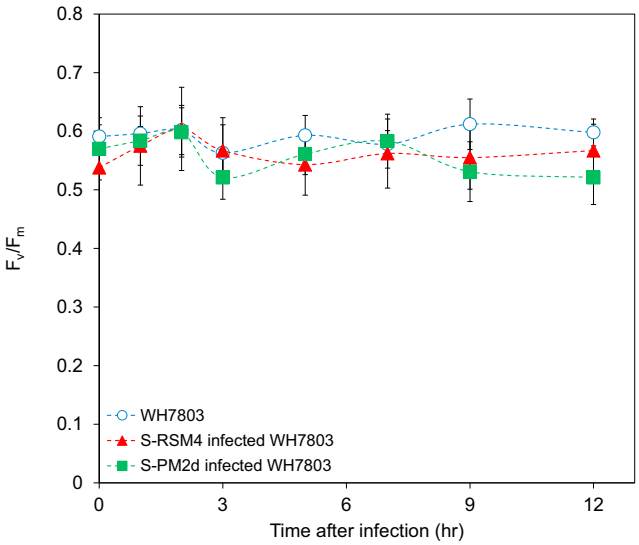

Figure 2. Photophysiological Parameters during Infection
Effective quantum yield of PSII photochemistry (F_v/F_M) measured over the infection period for uninfected *Synechococcus* sp. WH7803 and cells infected with S-PM2d and S-RSM4. Cells were incubated at 30 μmol photons m^{-2} s^{-1} in between measurements. Error bars represent the SD of the mean.

production tend to overestimate compared with ^{14}C in the open ocean [42], and while these deviations have been suggested to be explained by various cellular processes (see [43] for review), here we add another process that acts to consume photochemically generated electrons, ATP, and/or reductant at the expense of CO_2 fixation.

EXPERIMENTAL PROCEDURES

Infection Conditions

Synechococcus sp. WH7803 was grown in ASW medium in continuous light (25–30 μmol photons m^{-2} s^{-1}) at 23°C to an $OD_{750\ nm}$ between 0.35 and 0.40. Cell concentrations were measured using flow cytometry (FACScan, Becton Dickinson) and diluted to a concentration of 1 × 10^8 cells/ml with fresh ASW medium [44]. Samples were taken and either cyanophage S-PM2d or S-RSM4 was added to a virus-bacteria ratio (VBR) of 10 in triplicate. The virus titer was determined by plaque assay prior to the experiment as described in [45]. The samples were incubated at room temperature under low light (~25 μmol photons m^{-2} s^{-1}) for 1 hr to allow adsorption by cyanophages.

Measurement of CO_2 Fixation

CO_2 fixation rate measurements were made by assessing the amount of uptake of $NaH^{14}CO_3$ [46]. After cyanophage adsorption, cultures were diluted to a concentration of 1 × 10^7 cells/ml by addition of fresh ASW, and 0.1 MBq of $NaH^{14}CO_3$ (specific activity: 1.48–2.22 GBq/mmol, PerkinElmer) was added to each culture. In the first experiment (at a fixed light irradiance), the cultures were split into 3 ml volumes in clear polycarbonate tubes and incubated at 30 ± 5 μmol photons m^{-2} s^{-1}. The cultures were maintained at 23°C using a temperature-controlled water bath. An entire 3 ml culture was harvested at 1, 2, 4, 5, 7, and 9 hr post infection. In the second experiment, samples were again split into 3 ml volumes in clear polycarbonate tubes but were instead placed into a laboratory-built "photosynthetron," which acts to supply a gradient of light to experimental samples by placing them incrementally more distant from the light source [21]. Samples were incubated for 4 hr before being harvested. 4 hr was selected because previous experiments had shown that light significantly reduced the cyanophage latent period (unpublished data). Therefore, shortening the incubation period limited the effect of any early lysis in comparisons between phage and host and between phages. The light delivered to each polycarbonate tube was measured using a Spherical Micro Quantum US-SQS/B light meter (Walz), connected to a PhytoPAM (Walz). Once samples were taken, cells were fixed by addition of paraformaldehyde (final concentration 1%). Samples were acidified by addition of 0.5 vol 6N HCl in a

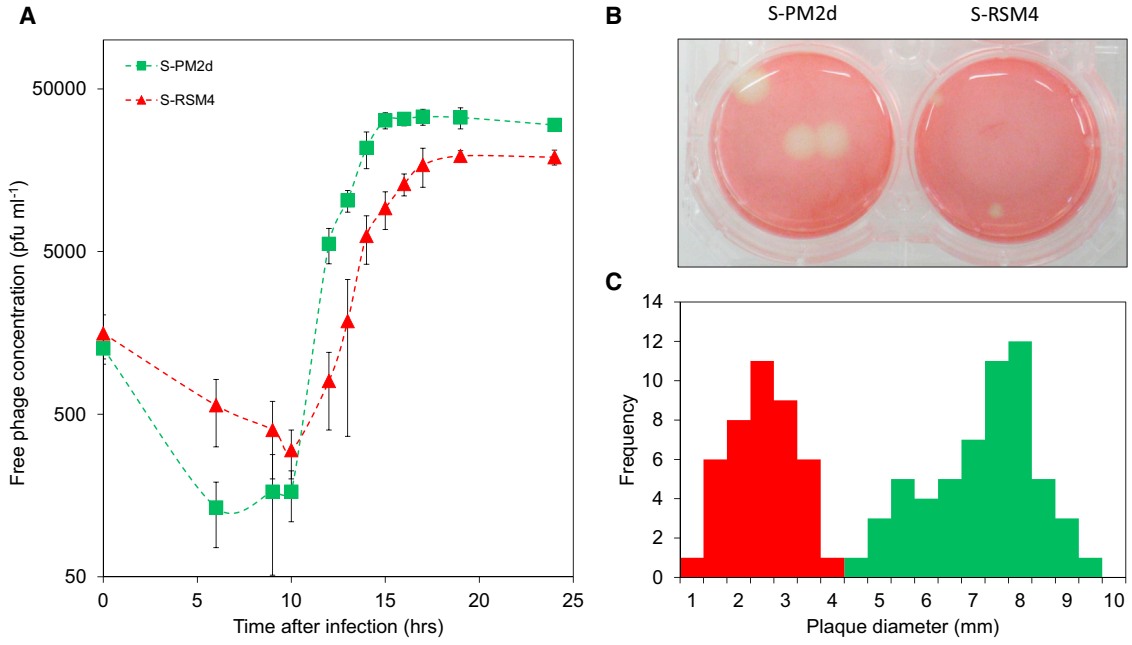

Figure 3. Phage Growth Parameters and Productivity Estimates
(A) One-step growth curves of S-PM2d and S-RSM4. Error bars represent the SD of the mean.
(B) Representative images of plaque sizes of S-PM2d and S-RSM4 after 10 days of growth.
(C) Frequency distributions of plaque diameters. Red bars indicate S-RSM4; green bars indicate S-PM2d.

Table 1. Photosynthesis Gene Copy Number of Cyanophages Used in This Study

			LH	Photosynthetic Electron Transport						Carbon Metabolism			
Phage	Isolation Site	Reference	*cpeT*	*psbA*	*psbD*	*hli*	*petE*	*petF*	*ptox*	*cp12*	*gnd*	*zwf*	*talC*
S-PM2d	English Channel	[26, 27]	1	1	1	2	–	–	–	–	–	–	–
S-RSM4	Red Sea	[19]	1	1	1	2	1	1	1	1	1	1	1

LH, light harvesting.

fume hood for 1 hr. Samples were then neutralized by addition of 0.5 vol 6N NaOH. 5 ml scintillation fluid (Ultima Gold, PerkinElmer) was added to scintillation vials and left overnight before scintillation counting using QuantaSmart software on a Packard Tri-Carb 2900TR scintillation counter.

Photophysiological Measurements

The effective quantum yield of PSII photochemistry (F_V/F_M) was measured following [47]. All measurements were made using a pulse amplitude-modulated fluorometer (PhytoPAM, Walz). Cells were incubated in the dark for 5 min to completely oxidize the primary electron acceptor Q_A. Weak modulating light was supplied at 520 nm at 1 μmol photons m^{-2} s^{-1} to measure basal fluorescence (F_0). Light-adapted maximal fluorescence (F_M) was measured in the presence of 100 μM 3-(3,4-dichlorophenyl)-1,1-dimethylurea (DCMU) following an ~30 s illumination of 1,300 μmol photons m^{-2} s^{-1} and a saturating pulse of 2,600 μmol photons m^{-2} s^{-1} for 200 ms. F_V/F_M was calculated as $(F_M\text{-}F_0)/F_M$.

One-Step Growth Curves and Phage Productivity Estimates

Synechococcus sp. WH7803 was grown to mid exponential phase. Cell concentration was determined by flow cytometry and cells were diluted in ASW to 1 × 10^7 cells/ml. S-PM2d and S-RSM4 were added to a VBR of 0.05 in triplicate and allowed to adsorb for 1 hr in continuous light. Subsequently the cultures were diluted 4,000-fold in ASW to synchronize infections and prevent reinfection of lysed virions. 100 μl were taken at specified intervals and centrifuged at 6000 × *g* for 10 min. The supernatant was taken and immediately titered by plaque assay following [45]. Phage productivity estimates were derived from relative plaque growth on a lawn of *Synechococcus* sp. WH7803. Phages were diluted to give an approximate yield of 1 phage per dilution. Subsequently, 10 μl was spotted in the center of a 6-well plate, and 200 μl of 10× concentrated *Synechococcus* sp. WH7803 (approximately 1 × 10^8 cells/ml) was mixed with the spot and left at room temperature for 1 hr. 2 ml of 0.35% (w/v) cleaned ASW agar [45] was mixed with the cell/phage mix by aspiration and allowed to cool. Plates were incubated for 10 days until plaques from both phages were visible. Plaque diameters were measured using ImageJ [48]. The latent period was calculated by testing for a significant increase (by t test) in the free phage concentration between each time point (after time point 0) and the time point with the lowest free phage concentration (i.e., immediately before lysis occurs). The burst size was calculated as the maximum free phage concentration divided by the minimum.

AUTHOR CONTRIBUTIONS

Conceptualization, R.J.P., A.D.M., D.J.E., and D.J.S.; Investigation, R.J.P; Writing – Original Draft, R.J.P; Writing – Review & Editing, R.J.P., A.D.M., D.J.E., and D.J.S.; Supervision, A.D.M, D.J.E., and D.J.S.

ACKNOWLEDGMENTS

R.J.P. was the recipient of a NERC studentship and Warwick University IAS fellowship. This work was supported in part by NERC grant NE/J02273X/1 and Leverhulme Trust grant RPG-2014-354 to A.D.M., D.J.E., and D.J.S.

Received: November 5, 2015
Revised: March 16, 2016
Accepted: April 13, 2016
Published: June 9, 2016

REFERENCES

1. Scanlan, D.J., Ostrowski, M., Mazard, S., Dufresne, A., Garczarek, L., Hess, W.R., Post, A.F., Hagemann, M., Paulsen, I., and Partensky, F. (2009). Ecological genomics of marine picocyanobacteria. Microbiol. Mol. Biol. Rev. *73*, 249–299.
2. Biller, S.J., Berube, P.M., Lindell, D., and Chisholm, S.W. (2015). *Prochlorococcus*: the structure and function of collective diversity. Nat. Rev. Microbiol. *13*, 13–27.
3. Flombaum, P., Gallegos, J.L., Gordillo, R.A., Rincón, J., Zabala, L.L., Jiao, N., Karl, D.M., Li, W.K., Lomas, M.W., Veneziano, D., et al. (2013). Present and future global distributions of the marine Cyanobacteria *Prochlorococcus* and *Synechococcus*. Proc. Natl. Acad. Sci. USA *110*, 9824–9829.
4. Field, C.B., Behrenfeld, M.J., Randerson, J.T., and Falkowski, P. (1998). Primary production of the biosphere: integrating terrestrial and oceanic components. Science *281*, 237–240.
5. Suttle, C.A., and Chan, A.M. (1993). Marine cyanophages infecting oceanic and coastal strains of *Synechococcus*: abundance, morphology, cross-infectivity and growth characteristics. Mar. Ecol. Prog. Ser. *92*, 99–109.
6. Waterbury, J.B., and Valois, F.W. (1993). Resistance to co-occurring phages enables marine *Synechococcus* communities to coexist with cyanophages abundant in seawater. Appl. Environ. Microbiol. *59*, 3393–3399.
7. Sullivan, M.B., Waterbury, J.B., and Chisholm, S.W. (2003). Cyanophages infecting the oceanic cyanobacterium *Prochlorococcus*. Nature *424*, 1047–1051.
8. Suttle, C.A., and Chan, A.M. (1994). Dynamics and distribution of cyanophages and their effect on marine *Synechococcus* spp. Appl. Environ. Microbiol. *60*, 3167–3174.
9. Suttle, C.A. (2007). Marine viruses–major players in the global ecosystem. Nat. Rev. Microbiol. *5*, 801–812.
10. Wilson, W.H., Carr, N.G., and Mann, N.H. (1996). The effect of phosphate status on the kinetics of cyanophage infection in the oceanic cyanobacterium *Synechococcus* sp. WH7803. J. Phycol. *32*, 506–516.
11. Lindell, D., Jaffe, J.D., Coleman, M.L., Futschik, M.E., Axmann, I.M., Rector, T., Kettler, G., Sullivan, M.B., Steen, R., Hess, W.R., et al. (2007). Genome-wide expression dynamics of a marine virus and host reveal features of co-evolution. Nature *449*, 83–86.
12. Mann, N.H., Cook, A., Millard, A., Bailey, S., and Clokie, M. (2003). Marine ecosystems: bacterial photosynthesis genes in a virus. Nature *424*, 741–742.
13. Lindell, D., Sullivan, M.B., Johnson, Z.I., Tolonen, A.C., Rohwer, F., and Chisholm, S.W. (2004). Transfer of photosynthesis genes to and from *Prochlorococcus* viruses. Proc. Natl. Acad. Sci. USA *101*, 11013–11018.
14. Sullivan, M.B., Coleman, M.L., Weigele, P., Rohwer, F., and Chisholm, S.W. (2005). Three *Prochlorococcus* cyanophage genomes: signature features and ecological interpretations. PLoS Biol. *3*, e144.
15. Sullivan, M.B., Huang, K.H., Ignacio-Espinoza, J.C., Berlin, A.M., Kelly, L., Weigele, P.R., DeFrancesco, A.S., Kern, S.E., Thompson, L.R., Young, S., et al. (2010). Genomic analysis of oceanic cyanobacterial myoviruses compared with T4-like myoviruses from diverse hosts and environments. Environ. Microbiol. *12*, 3035–3056.

16. Labrie, S.J., Frois-Moniz, K., Osburne, M.S., Kelly, L., Roggensack, S.E., Sullivan, M.B., Gearin, G., Zeng, Q., Fitzgerald, M., Henn, M.R., and Chisholm, S.W. (2013). Genomes of marine cyanopodoviruses reveal multiple origins of diversity. Environ. Microbiol. *15*, 1356–1376.

17. Philosof, A., Battchikova, N., Aro, E.-M., and Béjà, O. (2011). Marine cyanophages: tinkering with the electron transport chain. ISME J. *5*, 1568–1570.

18. Puxty, R.J., Millard, A.D., Evans, D.J., and Scanlan, D.J. (2015). Shedding new light on viral photosynthesis. Photosynth. Res. *126*, 71–97.

19. Millard, A.D., Zwirglmaier, K., Downey, M.J., Mann, N.H., and Scanlan, D.J. (2009). Comparative genomics of marine cyanomyoviruses reveals the widespread occurrence of *Synechococcus* host genes localized to a hyperplastic region: implications for mechanisms of cyanophage evolution. Environ. Microbiol. *11*, 2370–2387.

20. Thompson, L.R., Zeng, Q., Kelly, L., Huang, K.H., Singer, A.U., Stubbe, J., and Chisholm, S.W. (2011). Phage auxiliary metabolic genes and the redirection of cyanobacterial host carbon metabolism. Proc. Natl. Acad. Sci. USA *108*, E757–E764.

21. Johnson, Z.I., and Sheldon, T.L. (2007). A high-throughput method to measure photosynthesis-irradiance curves of phytoplankton. Limnol. Oceanogr. Methods *5*, 417–424.

22. Ginzburg, D., Padan, E., and Shilo, M. (1968). Effect of cyanophage infection on CO_2 photoassimilation in *Plectonema boryanum*. J. Virol. *2*, 695–701.

23. Sherman, L.A. (1976). Infection of *Synechococcus cedrorum* by the cyanophage AS-1M. III. Cellular metabolism and phage development. Virology *71*, 199–206.

24. Teklemariam, T.A., Demeter, S., Deák, Z., Surányi, G., and Borbély, G. (1990). AS-1 cyanophage infection inhibits the photosynthetic electron flow of photosystem II in *Synechococcus* sp. PCC 6301, a cyanobacterium. FEBS Lett. *270*, 211–215.

25. Lindell, D., Jaffe, J.D., Johnson, Z.I., Church, G.M., and Chisholm, S.W. (2005). Photosynthesis genes in marine viruses yield proteins during host infection. Nature *438*, 86–89.

26. Mann, N.H., Clokie, M.R.J., Millard, A., Cook, A., Wilson, W.H., Wheatley, P.J., Letarov, A., and Krisch, H.M. (2005). The genome of S-PM2, a "photosynthetic" T4-type bacteriophage that infects marine *Synechococcus* strains. J. Bacteriol. *187*, 3188–3200.

27. Puxty, R.J., Perez-Sepulveda, B., Rihtman, B., Evans, D.J., Millard, A.D., and Scanlan, D.J. (2015). Spontaneous deletion of an "ORFanage" region facilitates host adaptation in a "photosynthetic" cyanophage. PLoS ONE *10*, e0132642.

28. Tamoi, M., Miyazaki, T., Fukamizo, T., and Shigeoka, S. (2005). The Calvin cycle in cyanobacteria is regulated by CP12 via the NAD(H)/NADP(H) ratio under light/dark conditions. Plant J. *42*, 504–513.

29. Sullivan, M.B., Coleman, M.L., Quinlivan, V., Rosenkrantz, J.E., Defrancesco, A.S., Tan, G., Fu, R., Lee, J.A., Waterbury, J.B., Bielawski, J.P., and Chisholm, S.W. (2008). Portal protein diversity and phage ecology. Environ. Microbiol. *10*, 2810–2823.

30. Zinser, E.R., Lindell, D., Johnson, Z.I., Futschik, M.E., Steglich, C., Coleman, M.L., Wright, M.A., Rector, T., Steen, R., McNulty, N., et al. (2009). Choreography of the transcriptome, photophysiology, and cell cycle of a minimal photoautotroph, *Prochlorococcus*. PLoS ONE *4*, e5135.

31. Pelroy, R.A., Rippka, R., and Stanier, R.Y. (1972). Metabolism of glucose by unicellular blue-green algae. Arch. Mikrobiol. *87*, 303–322.

32. Kelly, L., Ding, H., Huang, K.H., Osburne, M.S., and Chisholm, S.W. (2013). Genetic diversity in cultured and wild marine cyanomyoviruses reveals phosphorus stress as a strong selective agent. ISME J. *7*, 1827–1841.

33. Kutter, E., Guttman, B., and Carlson, K. (1994). The transition from host to phage metabolism after T4 infection. In Molecular Biology of Bacteriophage T4, J.D. Karam, J.W. Drake, and K.N. Kreuzer, eds. (American Society for Microbiology), pp. 343–346.

34. Sharon, I., Tzahor, S., Williamson, S., Shmoish, M., Man-Aharonovich, D., Rusch, D.B., Yooseph, S., Zeidner, G., Golden, S.S., Mackey, S.R., et al. (2007). Viral photosynthetic reaction center genes and transcripts in the marine environment. ISME J. *1*, 492–501.

35. Baudoux, A., Veldhuis, M., Noordeloos, A., van Noort, G., and Brussaard, C. (2008). Estimates of virus- vs. grazing induced mortality of picophytoplankton in the North Sea during summer. Aquat. Microb. Ecol. *52*, 69–82.

36. Mojica, K.D.A., Huisman, J., Wilhelm, S.W., and Brussaard, C.P.D. (2015). Latitudinal variation in virus-induced mortality of phytoplankton across the North Atlantic Ocean. ISME J. *10*, 500–513.

37. Longhurst, A., Sathyendranath, S., Platt, T., and Caverhill, C. (1995). An estimate of global primary production in the ocean from satellite radiometer data. J. Plankton Res. *17*, 1245–1271.

38. Behrenfeld, M.J., O'Malley, R.T., Siegel, D.A., McClain, C.R., Sarmiento, J.L., Feldman, G.C., Milligan, A.J., Falkowski, P.G., Letelier, R.M., and Boss, E.S. (2006). Climate-driven trends in contemporary ocean productivity. Nature *444*, 752–755.

39. Polovina, J.J., Howell, E.A., and Abecassis, M. (2008). Ocean's least productive waters are expanding. Geophys. Res. Lett. *35*, L03618.

40. Cullen, J.J. (2001). Primary production methods. In Encyclopedia of Ocean Sciences, J.H. Steele, ed. (Academic Press), pp. 2277–2284.

41. Suggett, D.J., Moore, C.M., and Geider, R.J. (2011). Estimating aquatic productivity from active fluorescence measurements. In Chlorophyll *a* Fluorescence in Aquatic Sciences: Methods and Applications, D.J. Suggett, O. Prasil, and M.A. Borowitzka, eds. (Springer Science+Business Media), pp. 103–127.

42. Corno, G., Letelier, R.M., Abbott, M.R., and Karl, D.M. (2006). Assessing primary production variability in the North Pacific subtropical gyre: A comparison of fast repetition rate fluorometry and ^{14}C measurements. J. Phycol. *42*, 51–60.

43. Lawrenz, E., Silsbe, G., Capuzzo, E., Ylöstalo, P., Forster, R.M., Simis, S.G.H., Prášil, O., Kromkamp, J.C., Hickman, A.E., Moore, C.M., et al. (2013). Predicting the electron requirement for carbon fixation in seas and oceans. PLoS ONE *8*, e58137.

44. Wyman, M., Gregory, R.P.F., and Carr, N.G. (1985). Novel role for phycoerythrin in a marine cyanobacterium, *Synechococcus* strain DC2. Science *230*, 818–820.

45. Millard, A.D. (2009). Isolation of cyanophages from aquatic environments. In Bacteriophages: Methods and Protocols, Volume 1: Isolation, Characterization, and Interactions, Methods in Molecular Biology, M.R.J. Clokie, and A.M. Kropinski, eds. (Humana Press), pp. 33–42.

46. Steeman-Nielsen, E. (1952). The use of radioactive carbon (^{14}C) for measuring organic production in the sea. J. Cons. Perm. Int. Explor. Mer. *18*, 117–140.

47. Garczarek, L., Dufresne, A., Blot, N., Cockshutt, A.M., Peyrat, A., Campbell, D.A., Joubin, L., and Six, C. (2008). Function and evolution of the *psbA* gene family in marine *Synechococcus*: *Synechococcus* sp. WH7803 as a case study. ISME J. *2*, 937–953.

48. Abràmoff, M.D., Magalhães, P.J., and Ram, S.J. (2004). Image processing with ImageJ. Biophotonics Int. *11*, 36–42.